Acta Crystallographica Section D
Biological Crystallography
ISSN 0907-4449

Structure of human α-thrombin complexed with RWJ-51438 at 1.7 Å: unusual perturbation of the 60A–60I insertion loop

Rosario Recacha,[a] Michael J. Costanzo,[b] Bruce E. Maryanoff,[b] Mike Carson,[a] Lawrence DeLucas[a] and Debasish Chattopadhyay[a,c]*

[a]Center for Macromolecular Crystallography, University of Alabama at Birmingham, Birmingham, Alabama 35294-0005, USA, [b]The R. W. Johnson Pharmaceutical Research Institute, Spring House, Pennsylvania, USA, and [c]Division of Geographic Medicine, School of Medicine, University of Alabama at Birmingham, USA

Correspondence e-mail: debasish@cmc.uab.edu

Received 14 April 2000
Accepted 31 July 2000

PDB Reference: α-thrombin–RWJ-51438 complex, 1doj.

The three-dimensional structure of the ternary complex consisting of human α-thrombin, hirugen and the active-site inhibitor RWJ-51438 has been determined at 1.7 Å resolution. The crystals of the complex belong to the orthorhombic space group $P2_12_12$, with unit-cell parameters a = 62.98, b = 117.52, c = 47.99 Å. The refined R and R_{free} values are 0.196 and 0.232, respectively. The ketone carbonyl group of the inhibitor is covalently linked to the hydroxyl O atom of Ser195, forming a tetrahedral intermediate hemiketal structure; the benzothiazole ring N atom of RWJ-51438 forms a hydrogen bond with His57. Surprisingly, the carboxylate substituent on the benzothiazole group forms salt bridges with Lys60F NZ and the NZ of the symmetry-related residues Lys236 and Lys240, which introduces steric effects that perturb the 60A–60I insertion loop, especially at residues Trp60D and Phe60H.

1. Introduction

Thrombin is a serine protease that plays a central role in homeostasis and thrombosis (Blomback *et al.*, 1967; Mann, 1976; Berliner, 1992). One of the many important functions of thrombin is to catalyze the cleavage of fibrinogen to produce fibrin, which is a polymeric meshwork that stabilizes a blood clot resulting in a durable homeostatic plug (Davie *et al.*, 1991). Thrombosis can be regarded as a result of inappropriate thrombin activity. Consequently, thrombin is a potential therapeutic target for the treatment and prevention of thrombotic diseases.

α-Thrombin contains at least three areas of interaction with substrates and inhibitors (Fig. 1): (i) an active site comprising the catalytic triad (Ser195, His57 and Asp102) and the P1 specificity pocket that binds arginyl and lysyl side chains of substrate, (ii) a cationic fibrinogen-recognition exosite formed by residues Phe34–Leu40 and Arg73–Met84 at the bottom of a cliff-like wall that usually operates in concert with catalysis and (iii) an anion-binding exosite that is involved in heparin binding. This last site, which consists of the cationic residues Lys240, Lys233, Arg175, Arg101 and Arg93, also binds the second kringle domain of prothrombin through salt bridges.

A large number of inhibitor–thrombin complexes have been studied by X-ray crystallography (Pavone *et al.*, 1998), helping us to understand the roles that thrombin plays; however, little is known about the binding at the S′ sites. We are studying novel tripeptide transition-state analogues of the general form D-Phe-Pro-Arg-*X*, where *X* is a heterocyclic activating group. Two examples of such compounds are benzothiazoles I and II (Table 1). The use of a heterocycle at the P1′ position imparts the necessary electrophilicity to the arginine carbonyl moiety of the inhibitor (Edwards *et al.*, 1992;

Tsutsumi *et al.*, 1994; Costanzo *et al.*, 1996; Matthews *et al.*, 1996; Recacha *et al.*, 1999). An advantage of such heterocycle-activated ligands over those with other electrophilic ketones is the availability of heterocycles that can be incorporated into a peptidyl ketone, allowing modulation of the physiochemical properties.

We have determined the crystal structure of a complex of human α-thrombin with hirugen and the benzothiazole-containing inhibitor RWJ-51438 (II) at 1.7 Å resolution. The inhibitor, (*S*)-*N*-methyl-D-phenylalanyl-*N*-{4-[(aminoiminomethyl)amino]-1-[(6-carboxy-2-benzothiazolyl)carbonyl]butyl}-L-prolinamide trifluoroacetate hydrate (II), is a highly selective and potent inhibitor of thrombin ($K_i = 1.1 \pm 0.6$ n*M*). The structural differences between RWJ-50353–thrombin (Matthews *et al.*, 1996), which lacks a CO_2H substituent on the benzothiazole, and RWJ-51438–thrombin may explain the loss in thrombin affinity of RWJ-51438 (II) relative to RWJ-50353 (I) ($K_i = 0.14 \pm 0.03$ n*M*), despite the additional interactions in RWJ-51438–thrombin.

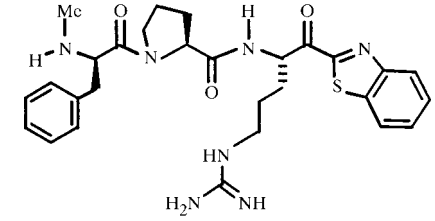

(I)

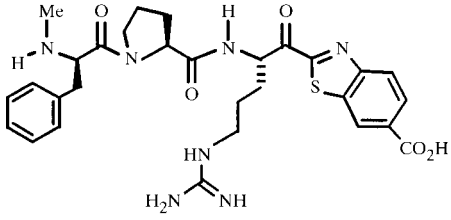

(II)

Here, we present the most important features of the human α-thrombin structure, its interactions with RWJ-51438 derived from the fully refined structure and its comparison with other thrombin complex structures.

2. Materials and methods

2.1. Crystallization

Frozen samples of human α-thrombin at a concentration of 1.12 mg ml^{-1} in 0.75 *M* sodium chloride solution were supplied by John W. Fenton (Fenton *et al.*, 1977). An approximately tenfold molar excess of hirugen, in the solid state, was added to a frozen 1 ml sample of thrombin and allowed to form complex for 2 h on ice and prevent the autolysis. The solution of the hirugen–thrombin complex was diluted to 2 ml with 50 m*M* phosphate buffer pH 7.3 and concentrated to about 6 mg ml^{-1} using a Centricon 10 mini-concentrator (MW cutoff 10 kDa) in a refrigerated centrifuge.

Table 1
Benzothiazole-activated thrombin inhibitors RWJ-50353 and RWJ-51438.

Compound	Structure	Thrombin K_i (n*M*)	Trypsin K_i (n*M*)
RWJ-50353	I	0.14 ± 0.03 ($n = 30$)	2.3 ± 1.1 ($n = 6$)
RWJ-51438	II	1.1 ± 0.6 ($n = 8$)	3.1 ± 0.07 ($n = 9$)

Concentrated thrombin–hirugen complex was incubated with a tenfold molar excess of RWJ-51438 for 2 h at 277 K. Crystallization was carried out at room temperature using the hanging-drop technique. Drops of 3 µl ternary complex solution mixed with 3 µl reservoir solution were equilibrated against 1 ml of well solution containing 0.1 *M* sodium cacodylate buffer pH 6.5, 0.75 *M* sodium acetate, 0.01%(*w*/*v*) sodium azide and 20%(*w*/*v*) polyethylene glycol 4000. Crystals suitable for X-ray diffraction, approximately 0.3 × 0.05 × 0.05 mm in size, were obtained after 5 d.

2.2. Data collection

X-ray diffraction data were collected at 103 K, using 25% glycerol in the reservoir solution as cryoprotectant, on an R-AXIS IV image plate and were processed with *DENZO* (Otwinowski & Minor, 1997). The completeness of data at 1.66 Å resolution is of 87.1%. The $R_{\rm merge}$ is 4% and the overall I/σ is 16.3.

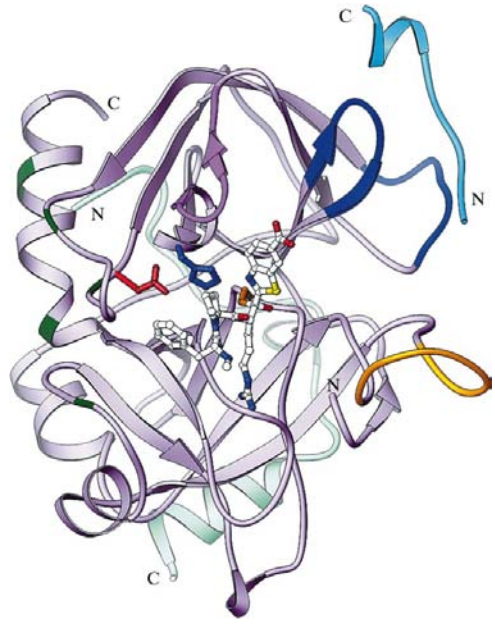

Figure 1
Ribbon drawing of the ternary complex thrombin–hirugen–RWJ-51438. The thrombin L-chain and hirugen ribbons are green and light blue, respectively. The thrombin H-chain is lavender with the insertion loop magenta. The cationic fibrinogen-binding loops on the right side (residues 34–40 and 73–84) and the heparin-binding residues (see text) on the left side are blue and the autolytic loop (residues 146–150) is gold. Side chains of the catalytic triad residues His57, Asp102 and Ser195 are blue, red and orange, respectively. The inhibitor is colored by atom type. All figures were prepared with *Ribbons* (Carson, 1997; http://www.cmc.uab.edu/ribbons) unless otherwise noted.

2.3. Structure determination and refinement

A search for the orientation and position of the thrombin molecule in the orthorhombic cell was performed using the program *AMoRe* (Navaza, 1994), diffraction data in the range 20–3.5 Å and the coordinates of a non-isomorphous thrombin–hirugen complex model (PDB code 1tmu; Priestle *et al.*, 1993). Fourier maps calculated after appropriate positioning of the thrombin molecule in the crystal cell allowed the rebuilding of the autolysis loop and addition of the omitted parts of the thrombin L-chain using the program *QUANTA*. The model of the thrombin–hirugen complex with uniform isotropic thermal (15.0 Å^2) and occupancy parameters was used for the initial refinement using *X-PLOR* (Brünger *et al.*, 1987). The RWJ-51438 inhibitor was located after the first round of refinement. Simulated annealing with slow cooling (Brünger *et al.*, 1990) and conjugate-gradient minimization were carried out. The refinement data were gradually extended to 1.7 Å resolution during the refinement. Solvent molecules were inserted at reasonable positions where the difference electron density exceeded 2.5σ. Finally, the individual atomic isotropic *B* factors were refined. Crystallographic statistics for the structure are reported in Table 2.

To provide a rigorous test for the accuracy of the model, omit maps covering a portion of the structure were computed following a simulated-annealing procedure in which coordinates of the portion of the model to be tested were removed (*X-PLOR*, v. 3.85). For the complex structure including 354 water molecules and two sodium ions, the *R* and R_{free} values are 19.6 and 23.2%, respectively, for 35 906 reflections (resolution limits 8–1.7 Å). The mean *B*-factor value for all atoms is 19.5 Å^2. The final atomic coordinates and structure factors have been deposited with the Protein Data Bank (RCSB number 010249; PDB code 1doj).

Table 2
Crystallographic data for human α-thrombin–RWJ-51483.

Space group	$P2_12_12$
Unit-cell parameters (Å)	a = 62.98, b = 117.52, c = 47.99
No. of reflections	289770
No. of unique reflections	42979
Reflections with $I > 3\sigma$ (%)	71
Overall completeness (99–1.66 Å) (%)	87
Completeness in the highest resolution shell (1.72–1.66 Å) (%)	43
R_{merge} (on I, overall) (%)	4
R_{merge} (highest resolution shell) (%)	20
$I/\sigma(I)$ overall	16.3
Refinement range (Å)	8–1.7
Number of reflections used in refinements	35906
R (%)	19.6
R_{free} (%)	23.2
R_{free} test set size (%)	4.5
R.m.s. deviation from standard	
Bond lengths (Å)	0.01
Bond angles (°)	1.39
Torsion angles (°)	26.42
Number of water molecules	354
Mean B value (all atoms) (Å^2)	19.5

3. Results and discussion

Crystals of the RWJ-51438–hirugen–thrombin ternary complex belong to the orthorhombic space group $P2_12_12$, with unit-cell parameters a = 62.98, b = 117.52, c = 47.99 Å. All the residues lie within the allowed regions of the Ramachandran plot with the exception of residue Phe7, which is in the generously allowed area.

3.1. Thrombin structure

The numbering of the thrombin residues used is based on topological equivalences with chymotrypsin (Hartley & Shotton, 1971). In this system, L-chain residues are numbered 1H–15 and H-chain residues are numbered 16–247, with insertions relative to the chymotrypsinogen structure numbered alphanumerically. The N-terminal residues of the L-chain of thrombin that precedes residue 1 in chymotrypsinogen are numbered in reversed alphanumerical order. The residues of hirugen are numbered 53′–64′, with 53′ designating the N-terminal Ac-Asn residue and 64′ designating the C-terminal Leu.

Electron density was well defined for most of the structure. The amino-terminal segment of the L-chain within the autolysis loop (Glu1C–Thr1H) and the C-terminus of the H-chain are only defined by relatively weak densities in the present structure and the amino-acid residues in these areas have been refined with occupancy lower than unity. These regions are typically found to be disordered in other thrombin complexes (Skrzypczk-Jankun *et al.*, 1991; Vijayalakshmi *et al.*, 1994). The weakly defined amino-terminal segment preceding Cys1 leans against a hydrophobic depression formed by Phe114 and Ile47 and extends with its amino-terminal residue 1H towards the carboxy-terminus of the L-chain. As is described in some

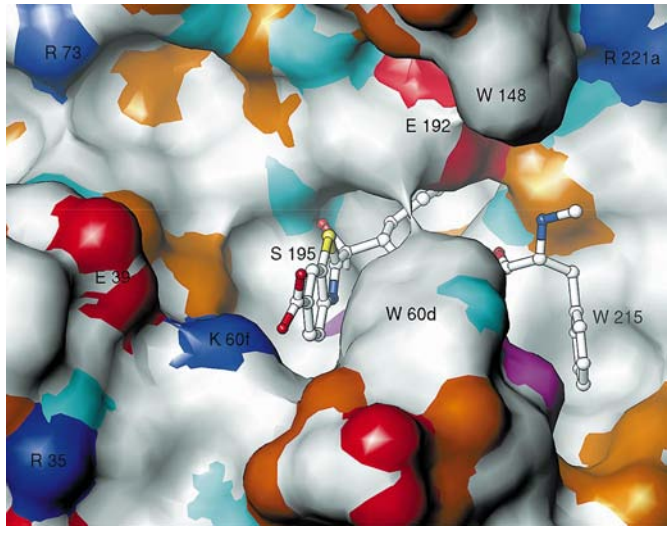

Figure 2
Surface of the active site colored by atomic chemical property. Positively charged atoms are blue, hydrogen-bond donors are cyan, negatively charged atoms are red, hydrogen-bond acceptors are orange, polar atoms (donators or acceptors) are magenta and hydrophobic atoms are white. The inhibitor is colored by atom type. Key surface residues are labelled.

Table 3
Distances of the hydrogen-bond interactions between RWJ-51438 and thrombin.

Protein	Inhibitor	Distance (Å)
Lys60F NZ	Bzt O1†	2.69
Lys236A NZ‡	Bzt O1	2.89
Lys240 NZ‡	Bzt O2	2.74
W963 O	Bzt O2	2.71
Ser195 N	Arg O	2.71
Gly193 N	Arg O	2.59
Asp189 OD1	Arg NH1	2.80
Asp189 OD2	Arg NH2	2.62
Gly219 O	Arg NH2	3.02
W533 O	Arg NH1	2.94
Ser190 O	Arg NH1	3.26
W589 O	Arg NE	2.86
Gly216 N	D-Phe O	2.94
Gly216 O	D-Phe N	2.77

† Benzothiazole moiety. ‡ Symmetry operator $x + \frac{1}{2}, -y + \frac{1}{2}, z$.

structures (Pavone *et al.*, 1998), the carboxyl-terminal segment Glu14C–Ser14I is organized as an amphiphilic α-helix, with its hydrophobic side (Val14B, Leu14E, Leu14G, Tyr14J) attached to the H-chain (Fig. 1).

The lytic loop containing Trp148 is generally well defined, being stabilized by the crystallographic contacts. As in the structure of thrombin with PPACK (D-Phe-Pro-Arg chloromethylketone; Bode *et al.*, 1992), the exposed loop lacks any inter-main-chain hydrogen bonds, but it is stabilized through hydrogen bonds made with the side chains of residues within the loop. In addition, some contacts with a symmetry-related molecule stabilize this loop in the present complex structure, as was observed in the PPACK–thrombin structure. The conformation of this loop in the present structure is different from that in the PPACK–thrombin complex. This loop exhibits a degree of flexibility (average B factor = 29 Å^2) in this structure. The present thrombin structure is similar to that of RWJ-50353–thrombin complex (r.m.s.d. C^α = 0.46 Å; PDB code 1tbz). The latter structure will be used throughout the text for comparison purposes.

The two N-terminal residues of hirugen (*N*-acetyl-Asn-Gly) are not observed in the electron-density map. The rest of the hirugen molecule from residue Asp55′ to Gln64′ is well defined. The interactions are comparable to those in the binary hirugen–thrombin complex (Bode *et al.*, 1992).

3.2. Active-site interactions

The active-site triad (Ser195, His57 and Asp102) shown in Fig. 1 is similar to that of the binary hirugen–thrombin complex structure (Vijayalakshmi *et al.*, 1994). The binding of the inhibitors in the active site does not significantly affect the overall structure of thrombin (Stubbs & Bode, 1993; De Simone *et al.*, 1998). Its groove extension is in fact created by a patch of positively charged side chains (Fig. 2), Lys36, Lys60F, Arg67, Arg75 and Arg77A. The last residue presents two distinct orientations in this structure.

The inhibitor RWJ-51438 is well defined in the electron-density map (Fig. 3). The binding of RWJ-51438 is similar to that of RWJ-50353; both belong to the PPACK class of inhibitors. The overall interactions between RWJ-51438 at the P1, P2 and P3 positions and thrombin are similar to complexes of thrombin with RWJ-50353 and PPACK (Matthews *et al.*, 1996).

To describe the interactions between thrombin and the inhibitor, the nomenclature introduced by Schechter & Berger (1967) is used. The position of the reactive site of the inhibitor is known as the primary binding site or P1 position. The Ser195 OG atom of thrombin forms a hemiketal intermediate with the carbonyl C atom of the P1 arginine of RWJ-51438, with a bond length of 1.4 Å. The geometry of the substituents around the carbonyl C atom is tetrahedral (Fig. 3), with the carbonyl O atom occupying the oxyanion hole, making hydrogen bonds with Gly193 N and Ser195 N (Table 3). The *N*-Me-D-Phe-Pro-Arg motif has all the interactions previously observed in inhibitor–thrombin complexes with this sequence binding in the active site (Fig. 4; Table 3). There is a doubly hydrogen-bonded ion pair of the P1 arginine guanidinium group with Asp189 in the S1 specificity pocket. In addition, one of the

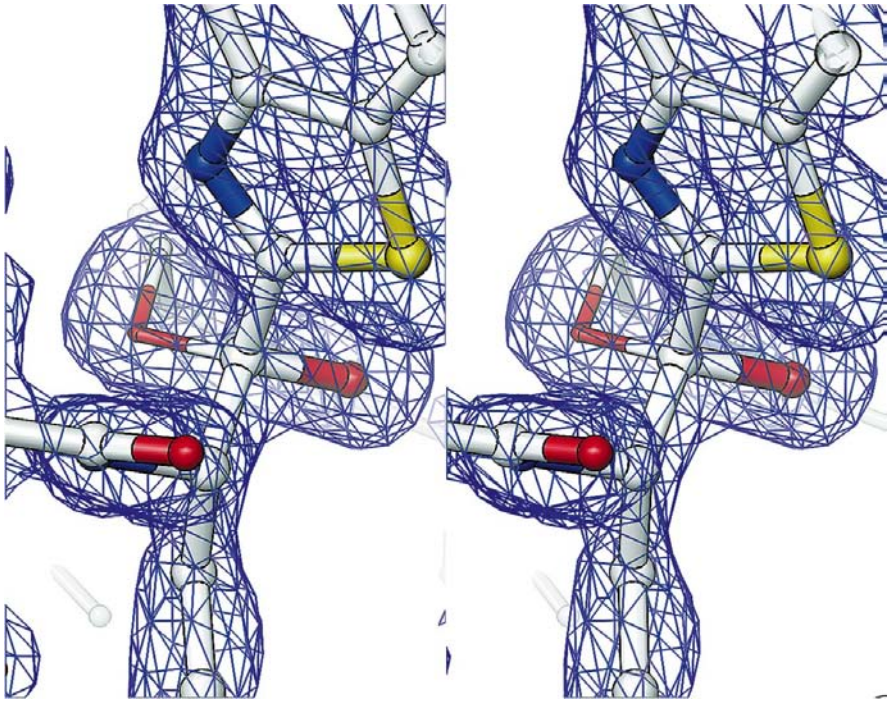

Figure 3
Stereoview of the electron-density map. A $2F_o - F_c$ map at 2.0σ is shown around the tetrahedral model of the thrombin–RWJ-51438 complex. The carbonyl group joined to the benzothiazole group of the inhibitor is covalently linked to the hydroxyl O atom of Ser195 (thinner bonds), forming a tetrahedral intermediate hemiketal structure.

N atoms of the guanidium group also interacts with Ala129 O and makes a water-mediated bridge to Phe227 O; the other N atom interacts with Gly219 O and two other water molecules. The NE atom of the guanidinium group forms a water-mediated hydrogen bond with Glu192 OE1, Gly219 O and Gly216 O. The inhibitor makes hydrophobic contacts with His57, Tyr60A, Trp60D and Leu99 in the S2 apolar site by its Pro residue and the formation of an antiparallel β-strand by the D-Phe-Pro-Arg sequence with the Ser214–Gly216 of thrombin (Bode *et al.*, 1989, 1992).

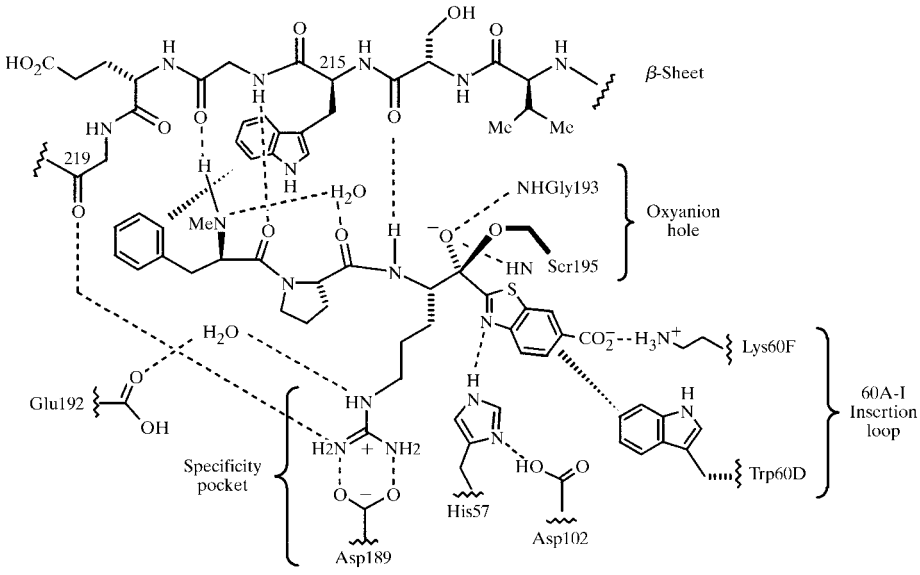

Figure 4
Diagram representing the key interactions between RWJ-51438 and thrombin.

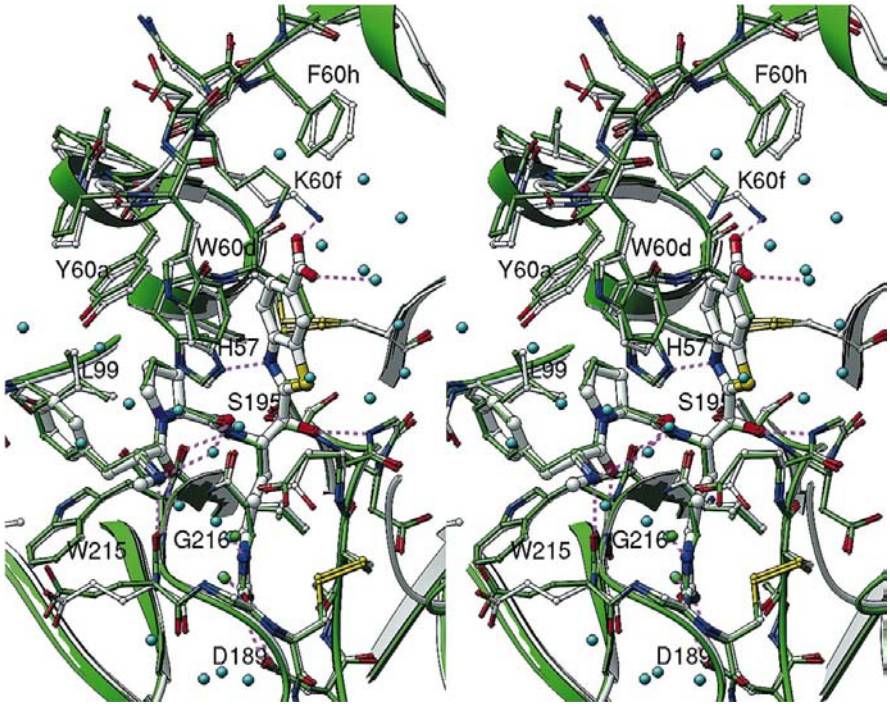

Figure 5
Stereoview of the thrombin–RWJ-51438 complex compared with the thrombin–RWJ-50353 complex. The RWJ-50353 complex is shown in the same manner, except the ribbon and all the C atoms are green.

3.3. P1′ interactions

The structures of thrombin complexes with thiazole inhibitors similar to RWJ-51438 have been reported. The comparison of RWJ-50353–thrombin (Matthews *et al.*, 1996; Costanzo *et al.*, 1996) and MOL-168–thrombin (Charles *et al.*, 1999) with the complex structure studied here shows similarities in the binding of the inhibitor to the protein. However, differences in binding of RWJ-51438 to thrombin are apparent owing to the presence of the carboxylate substituent on the benzothiazole (Bzt) ring. The active site of thrombin is particularly narrow when compared with other serine proteases of the same family. Hence, the presence of the carboxylate group in RWJ-51438 affects some residues of the 60A–60I insertion loop (Fig. 5), which is compact and somewhat rigid (Bode *et al.*, 1992).

A similar orientation was observed for the benzothiazole ring of the inhibitors RWJ-50353 (Matthews *et al.*, 1996) and MOL-168 (Charles *et al.*, 1999) complexed with thrombin. The thiazole S atom of the inhibitor points toward Glu192 and interacts with the amide N atom of Gly193 (3.5 Å). Residue Glu192, which is found in a flexible orientation in several thrombin–inhibitor complexes, is ordered in the present structure and interacts with the arginine residue of the inhibitor through a water-mediated hydrogen bond [NE—O(W589)—Glu192 OE1; Fig. 4, Table 3]. This residue seems to be crucial for stabilizing the inhibitor or the substrate in the active site (Pavone *et al.*, 1998). There is a hydrogen bond between His57 and the benzothiazole ring N atom which could delocalize the positive charge of a protonated N atom through the heterocyclic ring to the hemiketal O atom, resulting in further stabilization of the transition-state oxyanion (Edwards *et al.*, 1992).

The interactions of Lys60F appear to play an important role in the biological activity of thrombin (Wu *et al.*, 1991). The terminal side-chain

atoms of Lys60F in the structure of the RWJ-50353–thrombin complex curl away relative to the hirugen–thrombin complex in order to accommodate the bulky benzothiazole ring in the S1′ subsite (r.m.s.d. side chain = 1.564 Å). However, the carboxyl group joined to the benzothiazole ring forms a hydrogen bond with Lys60F NZ in the present structure. As a result, the displacement of the Lys60F side chain is not so pronounced. The amino group of the Lys60F does not form a hydrogen bond with the carbonyl O atom of His57. Usually, this particular hydrogen bond is formed when the S1′ subsite is either unoccupied or occupied by a small residue such as glycine (Bode *et al.*, 1992). The carboxylate group joined to the benzothiazole ring also forms a hydrogen bond with a water molecule (see Table 3) and forms a salt bridge with the NZ atoms of the symmetry-related residues Lys236 and Lys240.

Residues that form the groove joining the two functional sites of thrombin, especially the residues of the 60A–60I insertion loop, Trp60D and Phe60H, take different positions in the two complexes because of the presence of the carboxylate group in RWJ-51438 (Fig. 5). Whereas the non-bonded distance between the benzothiazole and the Trp60D in the present structure is shorter in comparison with the complex RWJ-50353–thrombin structure, leading to stronger van der Waals interactions, the remaining residues are more distant (Fig. 5). The S1′ subsite of thrombin generally accommodates smaller side chains as observed from the P1′ residues of a number of natural substrates (Qiu *et al.*, 1992). These residues include glycine and threonine and, in some cases, apolar residues such as Val15 of fibrinogen A, Leu13 of protein C and Ile153 and Ile37 of factor VII and factor XI, respectively (Tulinsky & Qiu, 1993; Tulinsky, 1996). The S1′ site is therefore capable of harboring moderately bulky side groups, although it appears to prefer smaller ones (Qiu *et al.*, 1992). The steric effects exerted by the carboxylate group may explain the higher K_i value of RWJ-51438 for thrombin than that of RWJ-50353. The perturbation of the insertion loop arises from a combination of effects of the negatively charged carboxylate ion that favor the approach of positively charged residues in its vicinity. This includes movement of the Lys60F toward the carboxylate end of the inhibitor.

This work was supported by funds from the R. W. Johnson Pharmaceutical Research Institute.

References

Berliner, L. J. (1992). Editor. *Thrombin: Structure and Function.* New York: Plenum Press.

Blomback, B. M., Blomback, B. H. & Iwanaga, S. (1967). *Nature (London)*, **215**, 1445–1448.

Bode, W., Mayr, I., Baumann, U., Huber, R., Stone, S. R. & Hofsteenge, J. (1989). *EMBO J.* **8**, 3467–3475.

Bode, W., Turk, D. & Karshikov, A. (1992). *Protein Sci.* **1**, 426–471.

Brünger, A. T., Krukowski, A. & Erickson, J. (1990). *Acta Cryst.* A**46**, 585–593.

Brünger, A. T., Kuriyan, J. & Karplus, M. (1987). *Science*, **2**, 458–460.

Carson, M. (1997). *Methods Enzymol.* **277**, 493–505.

Charles, R. S., Matthews, J. H., Zhang, E. & Tulinsky, A. (1999). *J. Med. Chem.* **42**, 1376–1383.

Costanzo, M. J., Maryanoff, B. E., Hecker, L. R., Schott, M. R., Yabut, S. C., Zhang, H. C., Andrade-Gordon, P., Kauffman, J. A., Lewis, J. M., Krishnan, R. & Tulinsky, A. (1996). *J. Med. Chem.* **39**, 3039–3043.

Davie, E. W., Fujikawa, K. & Kisiel, W. (1991). *Biochemistry*, **30**, 10363–10370.

De Simone, G., Lombardi, A., Galdiero, S., Nastri, F., Della-Morte, R., Staiano, N., Pedone, C., Bolognesi, M. & Pavone, V. (1998). *Protein Sci.* **7**, 243–253.

Edwards, P. D., Meyer, E. F. Jr, Vijayalaskhmi, J., Tuthill, P. A., Andisik, D. A., Gomes, B. & Stimpler, A. (1992). *J. Am. Chem. Soc.* **114**, 1854–1863.

Fenton, J. W. II, Landis, B. H., Walz, D. A. & Finlayson, J. S. (1977). *Chemistry and Biology of Thrombin*, edited by R. L. Lundblad, J. W. Fenton II & K. G. Mann, pp. 43–70. Ann Arbor: Ann Arbor Science.

Hartley, B. S. & Shotton, D. M. (1971). *The Enzymes*, edited by P. D. Boyer, Vol. 3, pp. 323–373. New York/London: Academic Press.

Mann, K. G. (1976). *Methods Enzymol.* **45**, pp. 123–156.

Matthews, J. H., Krishnan, R., Costanzo, M. J., Maryanoff, E. & Tulinsky, A. (1996). *Biophys. J.* **71**, 2830–2839.

Navaza, J. (1994). *Acta Cryst.* A**50**, 157–163.

Otwinowski, Z. & Minor, W. (1997). *Methods Enzymol.* **276**, 307–326.

Pavone, V., De Simone, G., Nastri, F., Galdiero, S., Staiano, N., Lombardi, A. & Pedone, C. (1998). *J. Biol. Chem.* **379**, 987–1006.

Priestle, J. P., Rahuel, J., Rink, H., Tones, M. & Grütter, M. G. (1993). *Protein Sci.* **2**, 1630–1642.

Qiu, X., Padmanabhan, K. P., Carperos, V. E., Tulinsky, A., Bode, W., Huber, R., Roitsch, C. & Fenton, J. W. II (1992). *Biochemistry*, **31**, 11689–11697.

Recacha, R., Carson, M., Costanzo, M. J., Maryanoff, B., DeLucas, L. J. & Chattopadhyay, D. (1999). *Acta Cryst.* D**55**, 1785–1791.

Schechter, I. & Berger, A. (1967). *Biochem. Biophys. Res. Commun.* **27**, 157–162.

Skrzypczk-Jankun, E., Carperos, V. E., Ravichandran, K. G., Tulinsky, A., Westbrook, M. & Maraganore, J. M. (1991). *J. Mol. Biol.* **221**, 1379–1393.

Stubbs, M. T. & Bode, W. (1993). *Thromb. Res.* **69**, 1–58.

Tsutsumi, S., Okonogi, T., Shibahara, S., Ohuchi, S., Hatsushiba, E., Patchett, A. A. & Christensen, B. G. (1994). *J. Med. Chem.* **37**, 3492–3502.

Tulinsky, A. (1996). *Semin. Thromb. Hemost.* **22**, 117–124.

Tulinsky, A. & Qiu, X. (1993). *Blood Coagul. Fibrinolysis*, **4**, 305–312.

Vijayalakshmi, J., Padmanabhan, K. P., Mann, K. G. & Tulinsky, A. (1994). *Protein Sci.* **3**, 2254–271.

Wu, Q. Y., Sheehan, J. P., Tsiang, M., Lentz, S. R., Birktoft, J. J. & Sadler, J. E. (1991). *Proc. Natl Acad. Sci USA*, **88**, 6775–6779.